Doughnut laser beam as an incoherent superposition of two petal beams

Igor A. Litvin,[1,5] Sandile Ngcobo,[1,2] Darry Naidoo,[1,3] Kamel Ait-Ameur,[4] and Andrew Forbes[1,2,3,6]

[1]*CSIR National Laser Centre, P.O. Box 395, Pretoria 0001, South Africa*

[2]*University of Kwazulu-Natal, Private Bag X54001, 4000 Durban, South Africa*

[3]*Laser Research Institute, University of Stellenbosch, Stellenbosch 7602, South Africa*

[4]*Centre de recherche sur les Ions, les Materiaux et la Photonique, UMR 6252 CEA-CNRS-ENSICAEN et Universite de Caen, CIMAP-ENSICAEN 6 Bd Marechal Juin, F-14050 Caen, France*

[5]*e-mail: ilitvin@csir.co.za*

[6]*e-mail: aforbes1@csir.co.za*

Received October 2, 2013; revised December 5, 2013; accepted December 8, 2013;
posted December 20, 2013 (Doc. ID 198641); published January 30, 2014

Laguerre–Gaussian beams with a nonzero azimuthal index are known to carry orbital angular momentum (OAM), and are routinely created external to laser cavities. The few reports of obtaining such beams from laser cavities suffer from inconclusive evidence of the real electromagnetic field. In this Letter we revisit this question and show that an observed doughnut beam from a laser cavity may not be a pure Laguerre–Gaussian azimuthal mode but can be an incoherent sum of petal modes, which do not carry OAM. We point out the requirements for future analysis of such fields from laser resonators. © 2014 Optical Society of America

OCIS codes: (140.3410) Laser resonators; (030.1640) Coherence; (140.3295) Laser beam characterization.
http://dx.doi.org/10.1364/OL.39.000704

Laguerre–Gaussian beams are well-known solutions to the Helmholtz equation under conditions of cylindrical symmetry, and a standard topic in many laser textbooks. Recently the azimuthal modes in the Laguerre–Gaussian basis have attracted renewed attention because they carry orbital angular momentum of $\ell\hbar$ per photon, where ℓ is the azimuthal index of the mode [1–3]. Numerous techniques have been developed for the generation of such beams external to the cavity by implementing spatial light modulators [4], spiral phase elements [5], cylindrical lens mode converters [6], and so on. There has also been considerable effort in creating such beams internal to the laser with an appropriate laser cavity. Techniques to achieve this have included thermally induced focusing [7,8], spatially variable retardation plates [9], and ring-shaped pumps [10,11]. In all the aforementioned examples an intensity pattern with a doughnut shape was observed from the cavity. Paradoxically this may not be indicative of the presence of an pure azimuthal Laguerre–Gaussian mode.

In this Letter we revisit the generation and detection of pure azimuthal Laguerre–Gaussian modes. We demonstrate a laser cavity that generates a doughnut-shaped mode and show by a series of experiments that it is not a pure Laguerre–Gaussian mode but rather an incoherent sum of petal-like modes. We illustrate that traditional tools for mode analysis, such as beam propagation and M^2 measurements, intensity, and second moment measurements, would not have been conclusive in determining the correct mode structure. Our results bring into question previous claims of Laguerre–Gaussian mode generation and outline the required analysis to overcome this ambiguity in future studies. Such structure of the doughnut mode may be in contradiction to the current experimental procedures of implementation, especially in areas such as optical tweezing of nanoparticles and atoms and angular-momentum-based experiments where it is necessary to know the real field structure and not only the intensity of the field.

We implement the selection of a doughnut-shaped mode through the use of an end-pumped solid-state laser configuration of the plano-concave variant, as in Fig. 1. An additional novelty is the use of a spatial light modulator (SLM) as a concave high reflector, thus forming the so-called "digital laser" [12]. The laser crystal (1% doped

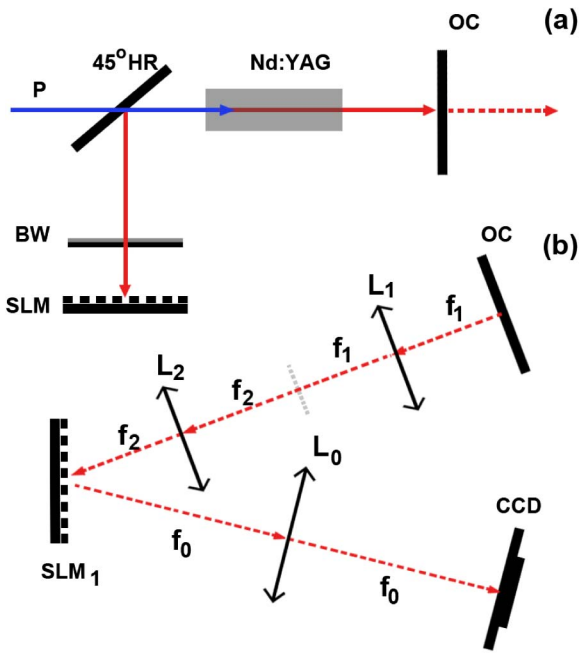

Fig. 1. (a) Schematic of the digital laser concept for the generation of a doughnut mode showing the spatial light modulator (SLM), Brewster window (BW), high reflectivity (HR) mirror at an angle of 45°, Nd:YAG gain medium pumped by an external laser diode (P) source, and the output coupler (OC). (b) Schematic of the experimental setup of the modal decomposition technique.

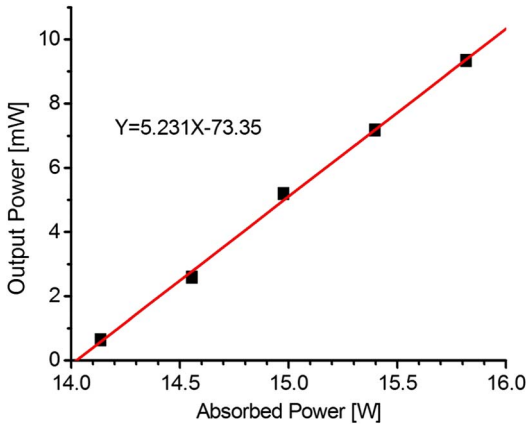

Fig. 2. Slope efficiency graph for generation of the doughnut mode by the digital laser setup.

Nd:YAG rod of 30 mm length and 4 mm diameter) was end pumped with a 75 W Jenoptik (JOLD 75 CPXF 2P W) multimode fiber-coupled laser diode operating at 808 nm. The laser mode size was selected for maximizing mode purity (i.e., avoiding aperture effects) and not output power, and consequently the threshold of the laser operation was achieved at an absorbed pump power of approximately 14 W with a slope efficiency of only 0.5% (see Fig. 2). We note that this could be made much higher with a cavity designed for maximizing output power; however, this was not the aim of the present study. The results were taken just above this threshold value and, hence, there were minimal thermal effects. Any disturbance to the stability of the system caused by the induced thermal lensing was compensated by curvature on the intracavity SLM and cavity length adjustment. The plane mirror was selected as the output coupler with a reflectivity of 60% for a cavity length of approximately 373 mm. The curvature of the concave mirror was digitally selected to be $R = 500$ mm, which gives rise to a g-parameter of 0.25, which is within the stability boundary $(0 < g < 1)$. The doughnut mode (Fig. 3) was selected by spot defecting the concave mirror with an opaque disk of radius $a = 0.5$ mm, where the curvature (phase) and opaque disk (amplitude) were encoded using complex amplitude modulation on the SLM [13]. The functionality of the laser is goverened by several key properties of the SLM (Hamamatsu, LCOS-SLM X110468E): high resolution (800×600) pixels each of 20 μm pitch, high efficiency at the desired polarization

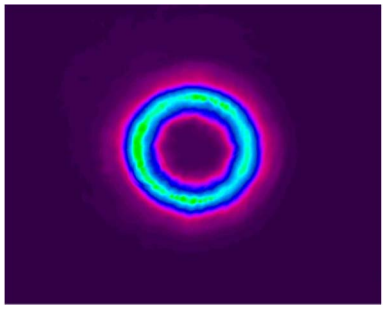

Fig. 3. Doughnut beam obtained by inserting an intracavity circular aperture into the conventional plano–concave stable cavity for implemention of the digital laser setup.

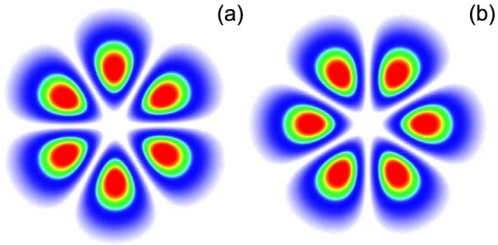

Fig. 4. Intensities of the modes with the highest eigenvalue, equivalent to 0.987, which was obtained through the Fox–Li method.

(90%), minimal phase–amplitude cross-talk, reasonable damage threshold (<30 W/cm^2), and a large phase shift (2π) at the laser wavelength. Further details of the operation of the digital laser can be found in [12,14].

We performed a Fox–Li analysis of the cavity using the parameters previously specified to identify the modal structure of the modes with the lowest round-trip losses. The intensity of the resulting modes with the highest eigenvalue, which corresponds to the lowest losses, is illustrated in Fig. 4.

We know from [15] that the obtained petal modes (see Fig. 4) are a superposition of two Laguerre–Gaussian modes of zero radial order $(p = 0)$ and azimuthal order ℓ and with different intermodal phase shift, namely,

$$u^{\ell}_{\text{even}}(r,\phi,z) = \text{LG}_{\ell}(r,\phi,z)[\exp(-i\ell\phi) + \exp(i\ell\phi)], \quad (1)$$

$$u^{\ell}_{\text{odd}}(r,\phi,z) = i\text{LG}_{\ell}(r,\phi,z)[\exp(-i\ell\phi) - \exp(i\ell\phi)], \quad (2)$$

where

$$\text{LG}_{\ell}(r,z,\phi) = \sqrt{\frac{2}{\pi w(z)^2|\ell|!}}\left(\frac{\sqrt{2}r}{w(z)}\right)^{|\ell|} \times \exp\left(-\frac{r^2}{w(z)^2} + ik_0\frac{r^2}{2R(z)}\right) \times \exp(i(1+|\ell|)\alpha(z)), \quad (3)$$

where $\alpha(z) = \arctan(z/z_r)$, $w(z) = w_0\sqrt{1+(z/z_r)^2}$, $R(z) = z(1+(z_r/z)^2)$, $z_r = \pi w_0^2/\lambda$, w_0 is beam width, and λ is the wavelength.

Based on the Fox–Li simulation and the experimental results we can assume that the obtained doughnut beam (see Fig. 3) is the superposition of two petal beams (see Fig. 4). Such a superposition can be generated by a coherent or incoherent sum of the petal beams [see Fig. 5 and Eqs. (4) and (5)]:

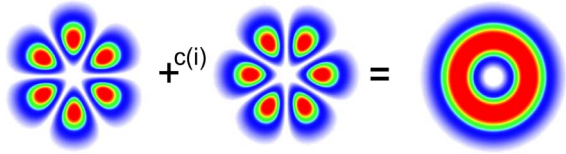

Fig. 5. Doughnut beam produced by a coherent and an incoherent superposition of the two petal beams.

$$D_i^{\ell}(r,z) = u_{\text{odd}}^{\ell}(r,\phi,z) +^{i} u_{\text{even}}^{\ell}(r,\phi,z), \tag{4}$$

$$D_c^{\ell}(r,z) = iu_{\text{odd}}^{\ell}(r,\phi,z) +^{c} u_{\text{even}}^{\ell}(r,\phi,z), \tag{5}$$

where $(+^c)$ is the coherent superposition and $(+^i)$ is the incoherent superposition.

Both the coherent and incoherent superposition will have the same final intensity distribution. However, we see that the final solution for the electromagnetic field of the coherent superposition [see Eq. (5)] is $D_c^{\ell}(r,z) = \text{LG}_{\ell}(r,z,\phi)\exp(i\ell\phi)$, which is in fact the field of a Laguerre–Gaussian mode [16]. This result is markedly different from an incoherent superposition where the two petal modes are treated independently, as all components are a superposition of two Laguerre–Gaussian modes of opposite azimuthal order [see Eq. (4)]. Based on this difference we are able to detect the correct solution for the superposition by applying an azimuthal modal decomposition technique [see Fig. 1(b)]. The modal decomposition was achieved by executing an optical inner product of the output beam with an azimuthal match filter [17]. The output beam from the laser was magnified by a $4f$ imaging system and directed onto SLM_1 [see Fig. 1(b)] to which the azimuthal match filter was addressed. The phase structure of the filter was set to $\exp(i\ell\phi)$ for various ℓ values. To identify the full set of azimuthal modes composing the output doughnut beam, an optical Fourier transform was performed of the resultant beam with the aid of a thin lens (L0) and the relative modal weightings were determined from the on-axis intensity [17,18].

In Fig. 6 we see the experimentally obtained modal decomposition of the doughnut mode. We see two peaks for the corresponding azimuthal mode numbers −3 and 3. This result is in contradiction to a coherent superposition as described in Eq. (5) as only a single peak is expected. We do, however, see that the modal decomposition is in perfect agreement with an incoherent superposition as described by Eq. (4) because the petal modes are treated independently and, thus, each mode would present two peaks [15,19].

To verify that the doughnut mode arrives from an incoherent superposition we have performed the following interference experiment (see Fig. 7). We direct the doughnut beam through a plate that consists of two

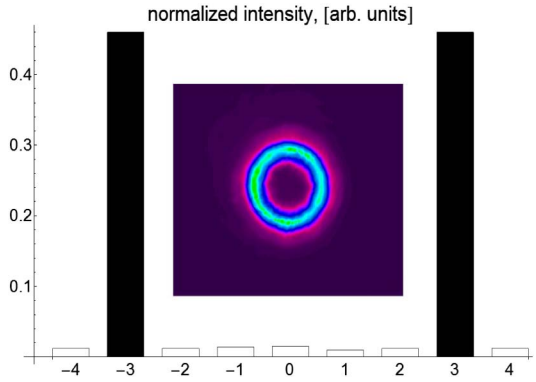

Fig. 6. Azimuthal modal decomposition of the doughnut mode.

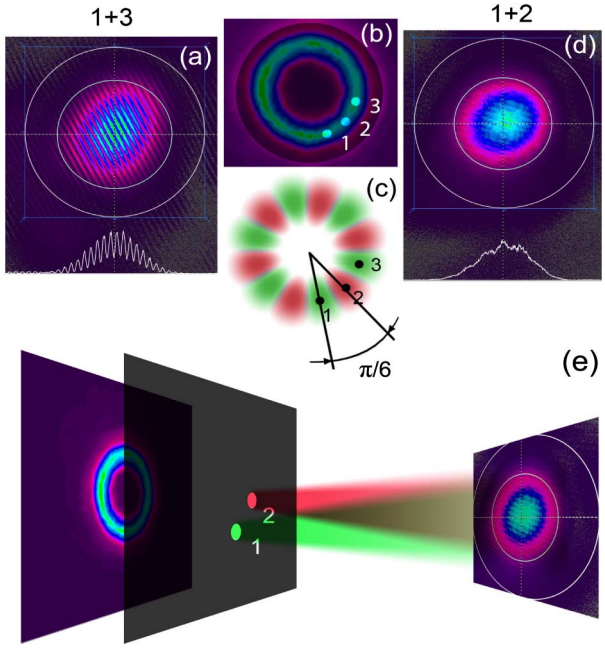

Fig. 7. Interference of the field produced by selecting two portions of the doughnut beam through two pinholes (b). The pinholes correspond to the lobes of the superimposed field (c), where we interfere either two lobes of the same petal beam [1 and 3, (a)] or two lobes with one from each petal beam [1 and 2, (d)]. (e) Schematic of the interference experiment.

pinholes. The positions of the pinholes corresponds to the positions of two of the petal lobes that comprise the superposition [see Fig. 7(c)]. The specific positions that we selected and their corresponding numbers are illustrated in Fig. 7(b). We thereafter directed the segments of the doughnut beam that passes through the pinholes to interfere at some position along the propagation axis [see Figs. 7(a), 7(d), and 7(e)].

The two petal fields that comprise the superposition for the doughnut beam are illustrated in Fig. 7(c) (green and red), and we expect that if we interfere lobes 1 and 2, we should see no interference fringes. However, if lobes 1 and 3 are interfered, then strong fringes will be present. This hypothesis is evident as is illustrated in Figs. 7(a) and 6(d) where notably stable interference lines are present.

The rigorous tests provided by the azimuthal modal decomposition and interference experiment are evidence enough to conclude that the doughnut mode is an incoherent superposition of two petal modes.

To understand the process occurring in the cavity during the modal buildup we have to take into account the area of the laser crystal that is pumped. Because of typical perturbations, it is not trivial to reach ideal symmetry from a custom laser cavity and there exists a degree of asymmetry. The asymmetry can be introduced through the geometry of the custom cavity or spatial distribution of the gain and presents a minimal difference in the eigenvalues of the two lowest loss modes, which were theoretically previously identical (petal modes, see Fig. 4). The lowest loss mode of the two will preferentially oscillate; however, the residual gain in the pumped medium will assist in the oscillation of the mode with the

higher round-trip losses. In the case of substantial asymmetry, the oscillation of the mode with higher losses becomes impossible and the output of the laser is a petal beam, which has previously been investigated in detail [15,20]. One may also understand this from a degeneracy perspective: since there is no physical process to distinguish the handedness of the pure azimuthal modes (positive or negative ℓ values), and since they have the same phase velocity and frequency, superpositions are easily formed—the well known petal modes.

In conclusion, we have made use of a novel digital laser capable of on-demand laser modes to output a doughnut mode. We have shown that, by using traditional techniques for characterizing the mode, we arrive at ambiguous conclusions. Contrary to previously reported studies, we perform a modal decomposition on our field that reveals it is not a pure Laguerre–Gaussian mode, but rather an incoherent mix of modes. Our theoretical analysis shows that doughnut-shaped modes may be produced by either coherent or incoherent mixing of odd and even petal-like modes, and that due care must be exercised to distinguish between the two cases. Our results bring into question previous reports on the generation of pure azimuthal Laguerre–Gaussian beams from such cavities, and outline a procedure for unambiguous predictions.

References

1. L. Allen, M. Beijersbergen, R. Spreeuw, and J. Woerdman, Phys. Rev. A **45**, 8185 (1992).
2. A. Mair, A. Vaziri, G. Weihs, and A. Zeilinger, Nature **412**, 313 (2001).
3. E. Yao, S. Franke-Arnold, J. Courtial, M. Padgett, and S. Barnett, Opt. Express **14**, 13089 (2006).
4. A. Shevchenko, S. Buchter, N. Tabiryan, and M. Kaivola, Opt. Commun. **77**, 232 (2004).
5. C. Paterson and R. Smith, Opt. Commun. **124**, 121 (1996).
6. M. W. Beijersbergen, L. Allen, H. E. L. O. van der Veen, and J. P. Woerdman, Opt. Commun. **96**, 123 (1993).
7. G. Machavariani, Y. Lumer, I. Moshe, A. Meir, S. Jackel, and N. Davidson, Appl. Opt. **46**, 3304 (2007).
8. M. Okida, Y. Hayashi, T. Omatsu, J. Hamazaki, and R. Morita, Appl. Phys. B **97**, 275 (2009).
9. G. Machavariani, Y. Lumer, I. Moshe, A. Meir, and S. Jackel, Opt. Commun. **281**, 732 (2008).
10. J. Kim and W. Clarkson, Opt. Commun. **296**, 109 (2013).
11. Y. Senatsky, J. F. Bisson, J. Li, A. Shirakawa, M. Thirugnanasambandam, and K. Ueda, Opt. Rev. **19**, 201 (2012).
12. S. Ngcobo, I. Litvin, L. Burger, and A. Forbes, Nat. Commun. **4**, 2283 (2013).
13. V. Arrizon, Opt. Lett. **28**, 2521 (2003).
14. S. Ngcobo, K. Ait-Ameur, I. A. Litvin, A. Hasnaoui, and A. Forbes, Opt. Express **21**, 21113 (2013).
15. D. Naidoo, K. Ait-Ameur, M. Brunel, and A. Forbes, Appl. Phys. B **106**, 683 (2012).
16. M. Harris, C. A. Hill, P. R. Tapster, and J. M. Vaughan, Phys. Rev. A **49**, 3119 (1994).
17. I. A. Litvin, A. Dudley, F. S. Roux, and A. Forbes, Opt. Express **20**, 10996 (2012).
18. C. Schulze, S. Ngcobo, M. Duparre, and A. Forbes, Opt. Express **20**, 27866 (2012).
19. I. A. Litvin, L. Burger, and A. Forbes, Opt. Lett. **38**, 3363 (2013).
20. I. A. Litvin, L. Burger, and A. Forbes, Opt. Express **15**, 14065 (2007).